Natural Convection From Dual Surface Heat Sources in a Vertical Rectangular Enclosure

الحمل الطبيعى من منبعين حراريين سطحيين فى حيز رأسى مستطيل

M.S. El-Kady
Mechanical Power Engineering Department
Mansoura University, Egypt

خلاصـــــة:

يتناول البحث دراسة نظرية وعملية لانتقال الحرارة بالحمل الطبيعى للهواء فى حيز ثنائى البعد رأسى مستطيل الشكل به منبعين حراريين (مسخنين) سطحيين ذات فيض حرارى ثابت ومثبتة على سطح رأسى معزول، بينما يبرد السطح الرأسى المواجه عند درجة حرارة ثابتة والسطحين الأفقيين معزولين. تكون النموذج من معادلات الاستمرار وكمية الحركة والطاقة واستخدمت طريقة الفروق المحددة للحل العددى. أجريت الدراسة على حيز مستطيل الشكل ذو $0.1\le S_1/H\le 0.5$, $0.1\le S_2/H_1\le 0.875$, $1\le A\le 10$, $10^4\le Ra\le 10^7$ و $Pr = 0.7$. أظهرت النتائج ان درجة الحرارة القصوى θ_{max} ومعامل انتقال الحرارة المتوسط $\bar{Nu}$ للمسخن السفلى لايتأثران بوضع المسخن العلوى أو بالنسبة الباعية عند $A\ge 3$. والمدى المثالى لموضع المسخن العلوى هو $S_2/H_1\le 0.6$ وفيه لايتأثر كل من θ_{max} و $\bar{Nu}$ بوضع المسخن العلوى أو بالنسبة الباعية عند $A\ge 3$. فى المدى المثالى لموضع المسخن السفلى $0.1\le S_1/H\le 0.5$ وموضع المسخن العلوى $S_2/H_1\le 0.6$ والنسبة الباعية $A\ge 3$ استنتجت علاقات تربط بين θ_{max} و $\bar{Nu}$ مع عدد رايلى كالتالى:

للمسخن السفلى: $\theta_{max} = 1.055\ Ra^{-0.139}$, $\bar{Nu} = 1.4\ Ra^{0.1179}$

للمسخن العلوى: $\theta_{max} = 1.4\ Ra^{-0.153}$, $\bar{Nu} = 0.99\ Ra^{0.135}$

أجريت دراسة عملية على حيز مستطيل ذو $A=2$, $S_1/H=0.2$. $S_2/H_1= 0.29$, $W/L=2.5$ $Ra=3.2\times10^4, 1.23\times10^5, 2.65\times10^5$ أظهرت نتائج الدراسة العددية توافقا جيدا مع النتاج العملية.

Abstract:

Natural convection in a heated two-dimensional rectangular vertical enclosure is investigated numerically and experimentally for different dual heater configurations. The governing couservation equations of mass, momentum, and energy for the problem are solved numerically using the finite difference technique. The study is carried out for the steady laminar flow of air in an enclosure with constant heat flux dual heaters at one adiabatic insulated vertical wall, an isothermally cooled other vertical wall and insulated horizontal walls. The range of parameters considered is $0.1\le S_1/H\le 0.5$, $0.1\le S_2/H_1\le 0.875$, $1\le A\le 10$. $10^4\le Ra\le 10^7$ and $Pr = 0.7$. The results show that for the lower heater θ_{max} and $\bar{Nu}$ are not affected by the location of the upper heater and the aspect ratio for $A\ge 3$. For the upper heater, θ_{max} and $\bar{Nu}$ are independent on the aspect ratio and the upper heater location in the optimum range of the upper heater location $S_2/H_1\le 0.6$ and $A\ge 3$. For the optimum ranges of the lower heater location $0.1\le S_1/H\le 0.5$, the upper heater location $S_2/H_1\le 0.6$ and the enclosure aspect ratio $A\ge 3$, θ_{max} and $\bar{Nu}$ are cortelated with Rayleigh number as follows:

for bottom heater: $\theta_{max} = 1.055\ Ra^{-0.139}$, $\bar{Nu} = 1.4\ Ra^{0.1179}$

for top heater: $\theta_{max} = 1.4\ Ra^{-0.153}$, $\bar{Nu} = 0.99\ Ra^{0\ 135}$

Experimental tests were done for $A=2$, $S_1/H= 0.2$, $S_2/H_1= 0.29$, $W/L=2.5$ and $Ra=3.2\times10^4, 1.23\times10^5$, and 2.65×10^5 and show the validity of the numerical simulation.

Accepted September 13, 1998

Introduction

In recent years, the study of natural convection in enclosures has become increasingly important. In particular, within the development of complex, high power electronics packaging and with the increasing demands on exhausting energy supplied, the understanding of free convective flows within rectangular enclosures heated by concentrated discrete heat sources has become warranted. In modern electronic equipments, a large number of high power dissipating components such as transistors, resistors, and power transformers are being packed in modular rectangular enclosures. The applications of these packages are often such that space, weight, and external cooling sources are minimal. In these cases, the placement of the high power dissipating components within an electronic package should be optimized as to maximize the natural convection heat transfer within the enclosure, thus possibly totally eliminating the need for forced cooling.

Extensive surveys of the various modes of convective heat transfer and relevant configurations along with the associated heat transfer and other correlations have been presented by Jaluria [1], Incropera [2], Papanicolaou and Jaluria [3] and El Kady and Araid [4]. Several works in the literature are dealing with mixed convection in the cooling of protruding heat sources of electronic components. among them the work of Habchi and Archarya [5], Kang et. al. [6], Mahaney et al. [7], Kim et. al. [8], and Papanicolaou and Jaluria [3]. Forced convection has been studied by many authors. Among them were Incropera et al. [9], Davalath and Bayazitoglu [10] and Kim and Anand [11-13], and Nakayama and Park [14]. Natural convection cooling techniques have distinct advantages because of their low cost, ease of maintenance and absence of electromagnetic interference and operating noise. Jaluria studied the buoyancy-induced flow due to isolated thermal sources on a vertical plate [15]. The natural convection between series of vertical plate channels with embedded line heat sources has been studied in order to meet the relatively lower operating temperature requirements of integrated circuits by Anand et al. [16], and Kim et al. [17,18]. Another important configuration involve complete and partial enclosures. Such as those that are encountered in small electronic devices and personal computers. Not much work has been done on such enclosure flows. But there is a growing interest in these problems. Keyhani et al. [19] investigated experimentally natural convection flow and heat transfer characteristics of an array of discrete heat sources in enclosures. and in [20] they showed the aspect ratio effect in natural convection. Carmona and Keyhani [21] showed the cavity width effect on cooling of five flush heaters on one vertical wall of an enclosure. El Kady and Araid [4] showed the effect of size and location of a surface heater embedded in the vertical wall of a two dimensional rectangular enclosure.

It is important to determine the extent of the wake region above the isolated heat sources, so that other components and surface heaters may be located without substantially reducing the heat transfer from them. The present study is directed to develop numerical model to investigate the heat transfer characteridtics due to the natural convection from two-dimensional discrete heat sources embedded in the vertical wall of the rectangular enclosures. It concentrates on the effect of the locations of the two heat sources, the enclosure aspect ratio and Rayleigh number on the surface temperature of the heat sources and the local and average heat transfer from them. Experimental test was done and the results were used to validate the numerical model.

Mathematical Formulation and Numerical Procedure

Two-dimensional steady laminar natural convection air flow is considered inside a vertical rectangular enclosure of height H and width W, as illustrated in Fig. 1. Two flat heat sources, with uniform heat flux input q and height L, are located on vertical adiabatic surface. The equations describing the problem are the Navier-Stokes equations for the fluid, with buoyancy effects taken into account and using the Boussinesq approximations, as well as the the energy equation, which describes the temperature variation through the enclosure (fluid and solid walls). With the introduction of the stream function and the vorticity as the independent variables, the nondimensional equations can be written as :

Vorticity Eq.: $$U.\partial\omega/\partial X + V.\partial\omega/\partial Y = \partial^2\omega/\partial X^2 + \partial^2\omega/\partial Y^2 + Ra/Pr.[\partial\theta/\partial X] \quad (1)$$

Stream function equation: $$-\omega = \partial^2\Psi/\partial X^2 + \partial^2\Psi/\partial Y^2 \quad (2)$$

Energy equation: $$U.\partial\theta/\partial X + V.\partial\theta/\partial Y = 1/Pr.[\partial^2\theta/\partial X^2 + \partial^2\theta/\partial Y^2] \quad (3)$$

where $$U=\partial\Psi/\partial Y \text{ and } V=-\partial\Psi/\partial X \quad (4)$$

ω is the dimensionless vorticity ($\omega=\partial V/\partial X-\partial U/\partial Y$), Ψ, θ, U, V, and ν are the dimensionless stream function, dimensionless temperature, dimensionless velocity in the dimensionless horizontal and vertical directions X and Y, and the fluid kinematic viscosity, respectively.

In the nondimensionalization, the height of the heater L, is taken as the characteristic length scale. The velocity scale is the L/ν, and the temperature scale is $\Delta T = q.L/k$. The dimensionless parameters are the Prandtl number $Pr = \nu/\alpha$ and the Rayleigh number $Ra = g\beta L^4 q/(k\alpha\nu)$. Where k, α, and β are the thermal conductivity, thermal diffusivity, and thermal expansion coefficient, respectively. More details for the formulation can be found in El Kady and Araid [4].

The dimensionless boundary conditions for the present system are

$$U = V = \Psi = 0, \text{ on all boundaries} \quad (5a)$$

$$\text{at } X = 0: \ \partial\theta/\partial X = -1 \text{ at heater surface, and } \partial\theta/\partial X = 0 \text{ elsewhere} \quad (5b)$$

$$\theta = 0 \text{ at } X = W/L, \text{ and } \partial\theta/\partial Y = 0 \text{ at } Y=0 \text{ or } H/L \quad (5c)$$

The local and average heat transfer coefficients along the surface of the heater are presented by means of Nusselt number and average Nusselt number according to its definition for isoflux heating as:

$$Nu = h.L/k = (q.L/k)/(T - T_w) \quad (6)$$

$$\bar{N}u = (q\,L/k)/(\bar{T} - T_w)] \quad (7)$$

where T_w and $\bar{T}$ are the cooling wall temperature and the average heater surface temperature, respectively. Nu and $\bar{N}u$ are the reciprocal of the dimensionless surface local and average temperatures, respectively.

The dimensionless governing equations (1)-(4) and the associated boundary conditions given by equation (5) were solved by a finite difference procedure discussed by Patanker [22]. Both the first and second order derivatives were discretized by using central difference formulas except the convection terms which were discretized by using the upwind scheme. The difference algebraic equations are solved using the Gauss-elimination method. An iterative solution proeedure was employed here to obtain the steady state solution of the problem considered. A non-uniform grid with

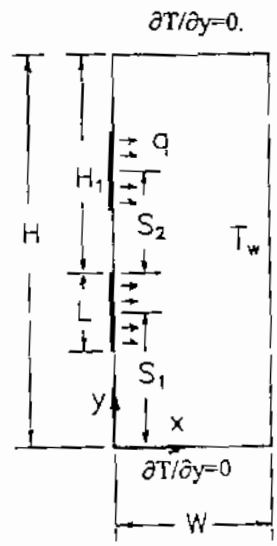

Fig. 1 Physical model, coordinate system and boundaries

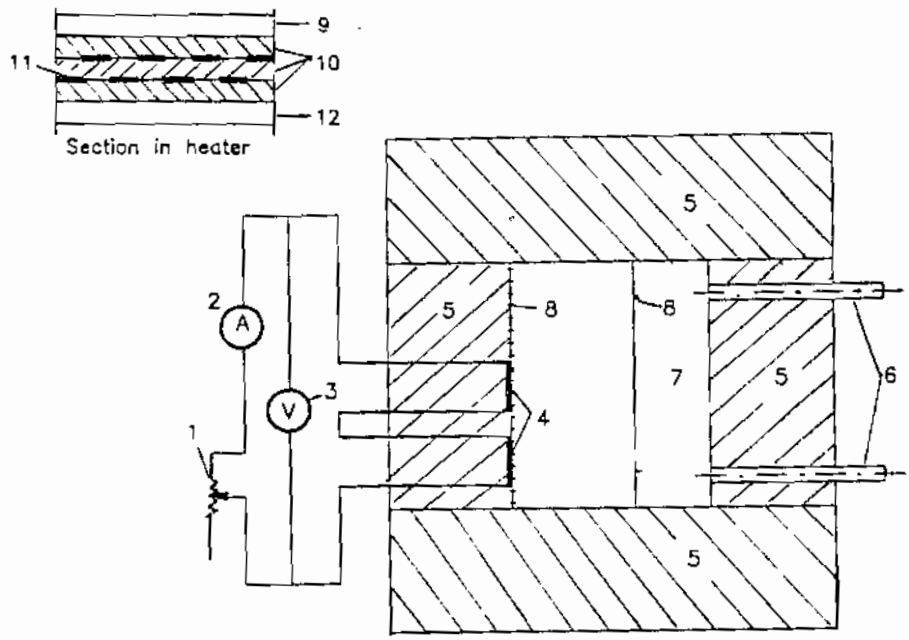

Fig. 2 Schematic diagram of the experimental apparatus

(1) auto transformer, (2) ammeter, (3) voltmeter, (4) electric heaters, (5) Polystyrene insulation, (6) inlet and outlet cooling water tubes, (7) Heat exchanger, (8) copper-constantan thermocouple, (9) stainless sheet plate, (10) sheet of mica, (11) nickel-chromium electric heater, (12) Thermal insulation layer

denser clustering near the walls was considered to give grid independent results. It varies from 41x41 for A=1 to 21x101 for A=10. The convergence criteria is attained when the relative error between two successive iterations for the field variables ω, Ψ, or θ is less than $\xi=10^{-5}$

Experimental Work:

To validate the program developed in this work an experimental study for the air flow in a rectangular enclosure is carried out. A schematic diagram of the designed and constructed apparatus is shown in Fig. 2. The used two dimensional rectangular enclosure is 100 mm height and 50 mm width and 300 mm in the spanwise direction. The right vertical wall of the enclosure was held at constant temperature by fitting a copper counter-flow heat exchanger (7) in which the city water was used as a coolant liquid. The two horizontal surfaces were maintained adiabatic by conducting them of closed-pore extruded polystyrene insulation with 50 mm thickness. The left vertical wall of the enclosure was made of the closed-pore extruded polystyrene insulation (5) of 50 mm thickness. Two electric heaters (4) with dimensions of 20 mm height, 2.5 mm thickness, and 300 mm long was embedded in the left vertical adiabatic wall to make the heater face in the same vertical inside plane of the wall. The vertical distances between the two heaters was 10 mm, between the bottom horizontal wall and the lower heater was 10 mm and between the upper heater and the top horizontal wall was 40 mm. Each heater face is made of polished stainless steel sheet (9) with 0.5 mm thickness. This sheet was heated electrically by an electric heater. A nickel-chromium wire (11) was wounded around a mica sheet (10) of 0.5 mm thickness and then was sandwiched between other two mica sheets (10). The heat input to the heaters was controlled by using an auto-transformer (1), an ammeter (2) and voltmeter (3).

The temperature distribution along the heated and unheated parts of the vertical wall was measured by 24 copper-constantan thermocouples. 20 thermocouples were fixed in the middle plane of the spanwise as shown in Fig. 2. The other 4 thermocouples were fixed in the middle height of each stainless sheet at 100 mm distance in both sides from the middle plane of the spanwise. Two thermocouples (8) were embedded in the wall of the heat exchanger (7) and monitored to ensure a uniform temperature distribution. The thermocouples were connected to digital temperature recorder. Nearly three hours were needed to reach the steady state condition which was recorded, as the temperature reading did not change within a time of about 15 minutes.

Results and Discussion

A careful examination of the model equations and the associated boundary conditions reveals that the independent parameters are the fluid Prandtl number Pr, the Rayleigh number Ra, the aspect ratio A=H/W, the location of the lower heater S_1/H, and the wake distance between the upper and lower heater, S_2/H_1. El Kady and Araid [4] concluded that the optimum location for a single heater in a vertical enclosure corresponding to maximum heat transfer and minimum surface temperature lies in the

range of $0.1 \le S_1/H \le 0.5$, i.e. in the lower half of the enclosure. Therefore, the location of the lower heater is chosen to be in this optimum range in the present study. For the value of Pr=0.7, the present study concentrates on the effect of the variation of the upper heater location (wake distance between upper and lower heaters) $0.125 < S_2/H_1 \le 0.875$, the variation of the aspect ratio $1 \le A \le 10$, and the variation of Rayleigh number $10^4 \le Ra \le 10^7$ on the flow and heat transfer characteristics to get the optimum position for the upper heater corresponding to the maximum heat transfer and minimum heater surface temperatures and correlations which describes these variables.

Effect of the upper heater location

The heat transfer from the heaters and the surface temperatures of them depend mainly on the velocity and temperature of the air flowing in the adjacent boundary layer. So, the qualitative prediction of the behaviour of the streamlines and the isothermal contours inside the enclosure is necessary

Figure 3 presents the streamlines and temperature contours for $S_1/H = 0.1667$, $Ra = 10^5$ with the variation of the upper heater location relative to the lower heater $S_2/H_1 = 0.2$, 0.3, 0.4, 0.6 and 0.8. Near the heated section along the hot wall and the opposing vertical wall thick layers of primary flows are observed in Fig. 3a. Between these layers exists a long core flow. The core flow starts from the low region of the lower heater and ends near the top surface of the enclosure. For $S_2/H_1 = 0.8$ the upper heater moves nearer to the top of the enclosure, secondary cell in front of the upper heater exists, which in turns causes a decrease in the maximum stream function and the flow velocity in front of the upper heater. As shown in Fig. 3b, a growth of the thermal boundary layer along the two heaters exists. The temperature distribution for the core fluid and the cold wall is nearly constant with the exception of the top section of the enclosure. In the top section of the enclosure the temperature increases as the upper heater moves towards the top horizontal adiabatic surface. The temperature in front of the lower heater is nearly constant and independent on the location of the upper heater.

Fig. 4 shows the temperature distribution at the hot wall for the heated and unheated sections, while Fig. 5 presents the local Nusselt number for both heaters for $S_1/H = 0.1667$, $Ra = 10^5$ and $S_2/H_1 = 0.4$, 0.6 and 0.8. The above characteristics of the streamlines and isotherms inside the enclosure reveals that the air coming from the cooled wall and entering the leading edge of the lower heater is nearly at constant temperatures for all considered cases. Therefore, the surface temperature and the local Nu of the lower heater is constant for the four cases. the surface temperature of the lower heater is smaller than that of the upper heater, and the local Nusselt number for the lower heater is higher than that of the upper heater for the four cases considered in Figs. 4 and 5.

The influence of the upper heater location (wake distance) $0.125 < S_2/H_1 \le 0.875$ on the maximum surface temperatures and the average Nusselt number for both heaters are presented in Figs. 6 and 7. The maximum surface temperature θ_{max} for the lower heater is smaller than that of the upper heater while $\overline{Nu}$ is higher than that of the upper heater. For the lower heater both the maximum surface temperature θ_{max} and the average Nusselt number $\overline{Nu}$ are not affected by the location of the upper heater (the variation of S_2/H_1). For the upper heater, with the increase of S_2/H_1 (the wake

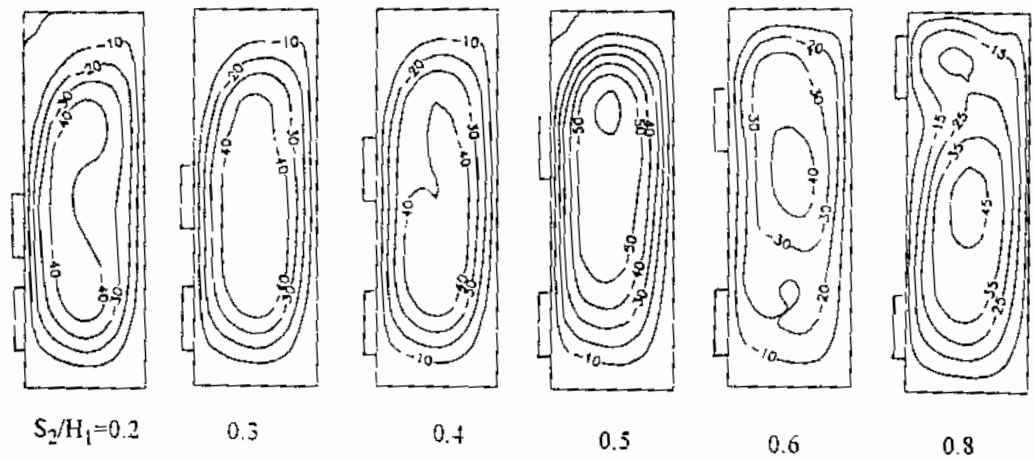

(a) Stream Pattern

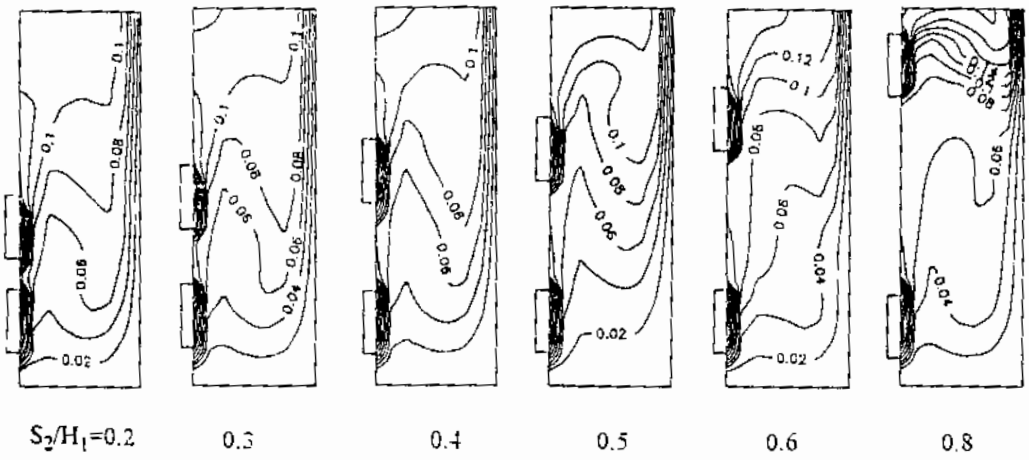

(b) Isotherms Contours

Fig. 3 Stream pattern and isotherm contours for different upper heater locations, Pr =0.7, S_1/H=0.1667, A=3, and $Ra=10^5$

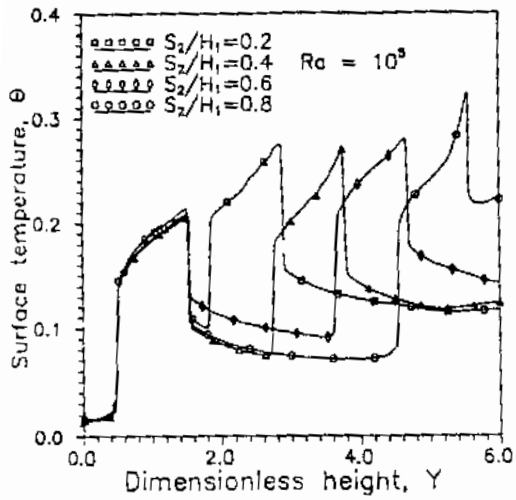

Fig. 4 Surface temperature distribution for different upper heater locations, Pr =0.7, S_1/H=0.1667, A=3, and Ra=10^5

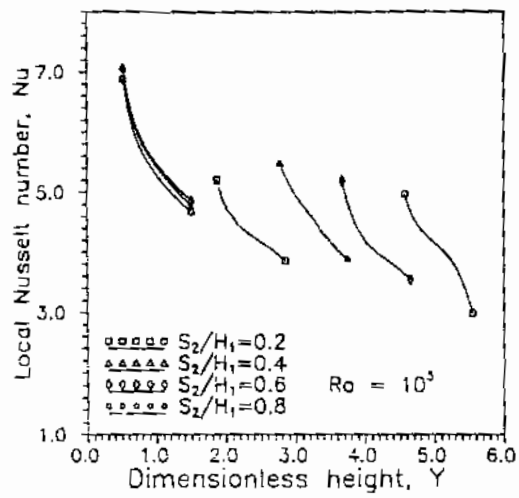

Fig. 5 Local Nusselt Number variation for different upper heater locations, Pr = 0.7, S_1/H=0.1667, A=3, and Ra=10^5

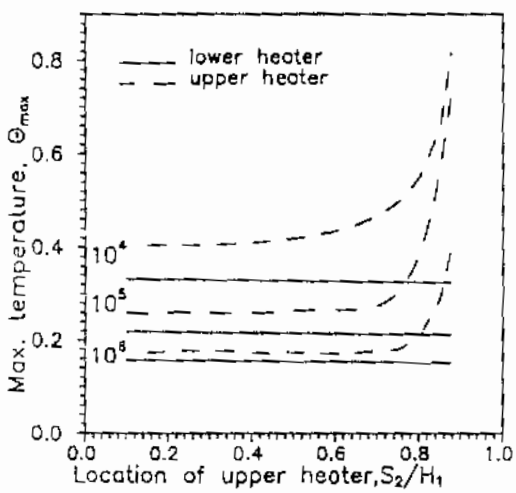

Fig. 6 Influence of upper heater locations on the maximum surface temperature for Pr =0.7, S_1/H=0.1667, A=3

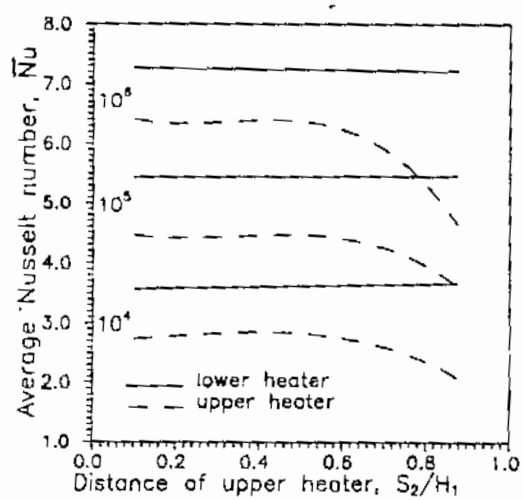

Fig. 7 Influence of the upper heater locations on the average Nusselt number for Pr=0.7, S_1/H=0.1667, A=3

distance increases), both θ_{max} and $\bar{N}u$ are independent on the upper heater location and are nearly constant until $S_2/H_1 = 0.6$. For $S_2/H_1 \geq 0.6$, the upper heater becomes nearer to the top surface, the maximum stream function in front of it decreases and the air flow passing through the adjacent boundary layer becomes slower with increasing temperature. For those reasons, the maximum surface temperature θ_{max} increases sharply and the average Nusselt number $\bar{N}u$ sharply decreases. Therefore, the optimum location for the upper heater corresponding to maximum average heat transfer $\bar{N}u$ and minimum surface maximum temperature θ_{max} lies in the lower half of the distance above the trailing edge of the lower heater where $S_2/H_1 \leq 0.6$.

Effect of Aspect Ratio

Figure 8 presents the streamlines and isothermal contours with the variation of aspect ratio $2 \leq A \leq 8$ for $Ra = 10^5$, while Figs. 9 and 10 present the variation of the maximum surface temperature and average Nusselt number for both the lower and upper heaters with the variation of the aspect ratio $1 \leq A \leq 10$ for $Ra = 10^4$, 10^5, and 10^6. In Figs 8-10 both heaters lie in the optimum location range with $S_1/H = 0.1667$ and $S_2/H_1 = 0.3$. As shown in Fig. 8a, thick layers of primary flow are observed near the hot and opposing vertical walls. With the increase of the aspect ratio a long and narrow core flow exists between the primary flow with disappearing of the secondary core flow cells. A secondary recirculating zone with low intensity can be predicted in the upper left corner indicating the separation of the flow originating from the top heater and rising along the remainder of the adiabatic wall. Although higher maximum streamfunctions appear with the increase of aspect ratio, the maximum values of streamfunctions are nearly constant for $A \geq 3$ in front of each heater which means nearly constant flow velocity inside the enclosure in front of each heater. Fig. 8h shows that with the increase of the aspect ratio, the active height of the isothermal cold wall increases and the chance to transfer more heat from the heater to the cold wall increases. By the Aspect ratio $A \geq 3$, the temperature of the core flow in front of each heater and temperature in the boundary layer adjacent to them are nearly constant. For the above reasons the air adjacent to the heaters flows with nearly constant velocity and temperature, and both the average Nusselt number and the maximum surface temperatures for both the lower and upper heaters are nearly constant and independent on the Aspect ratio for $A \geq 3$ as shown in Figs. 9 and 10. The same behaviour of the average Nusselt number and maximum surface heater temperatures exist for different values of Rayleigh number: $Ra = 10^4$, 10^5, and 10^6.

Effect of Rayleigh number

For constant Rayleigh number, Figs. 7 and 8 show that, the maximum surface temperature and the average Nusselt number of both the lower and upper heaters are independent on S_2/H_1 for the range of $S_2/H_1 \leq 0.6$, while Figs. 9 and 10 present also that the maximum surface temperature and average Nusselt number of both the lower and upper heaters are independent on enclosure aspect ratio for the range of $A \geq 3$.

For the optimum range of the lower heater location $0.1 \leq S_1/H \leq 0.5$, the optimum range of upper heater location $S_2/H_1 \leq 0.6$ and the optimum range of enclosure aspect

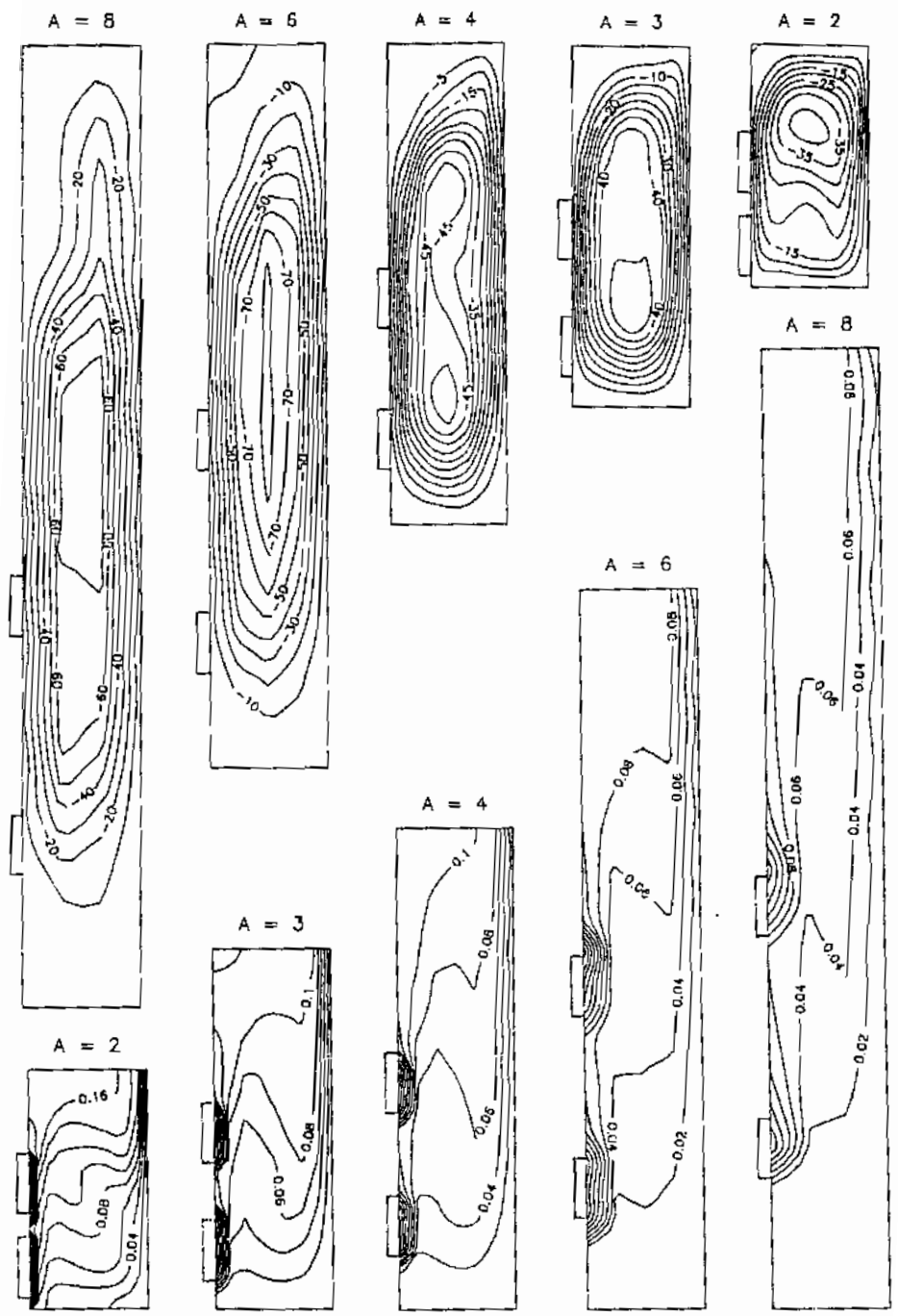

Fig. 8 Stream pattern and isotherm contours for different enclosure aspect ratios, Pr =0.7, S_1/H=0.1667, S_2/H_1=0.3, and Ra=10^5

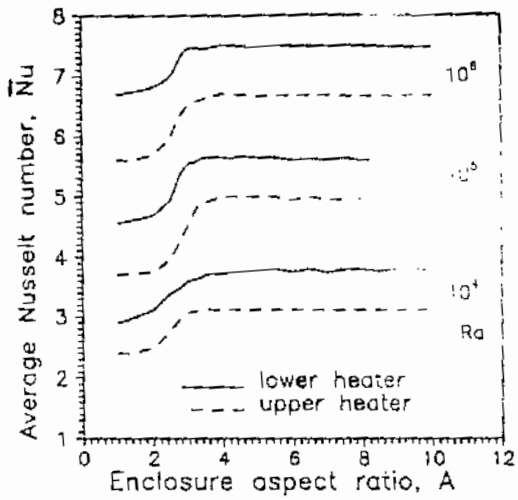

Fig. 9 Influence of enclosure aspect ratio on the average Nusselt number for Pr = 0.7, S_1/H=0.1667, S_2/H_1=0.3

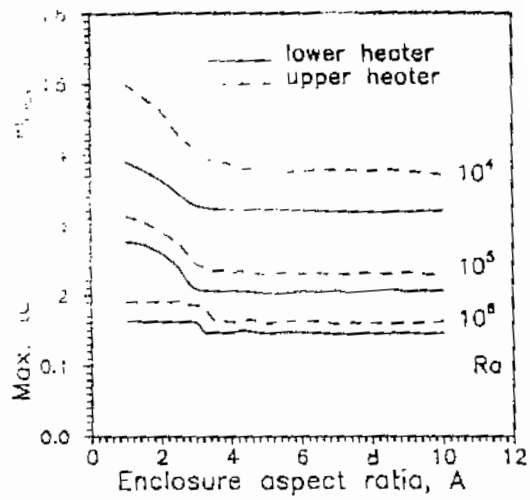

Fig. 10 Influence of enclosure aspect ratio on the maximum surface temperature for Pr = 0.7, S_1/H=0.1667, S_2/H_1=0.3

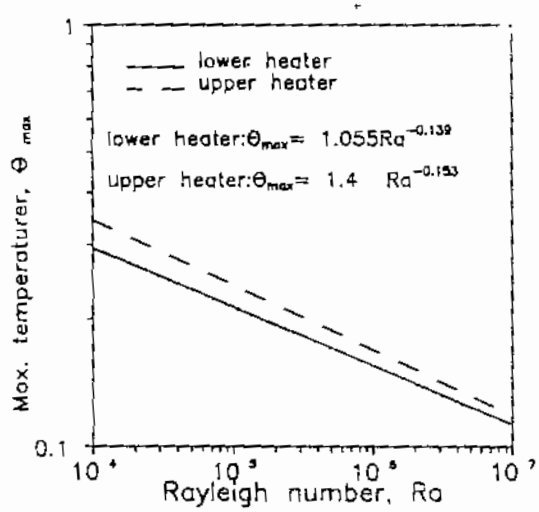

Fig. 11 Influence of Rayleigh number on the maximum surface temperature for Pr = 0.7, $0.1 \le S_1/H \le 0.5$, $S_2/H_1 \le 0.6$, and $A \ge 3$

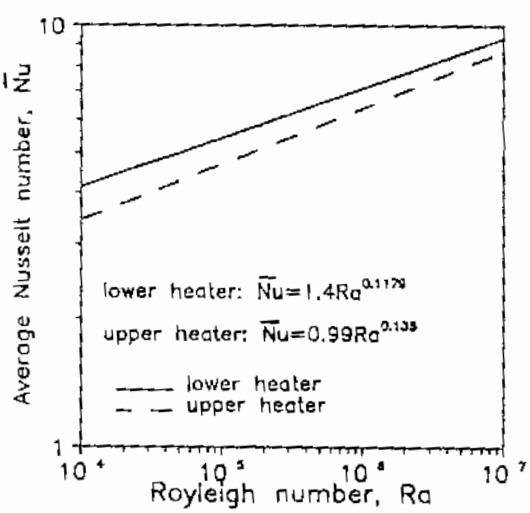

Fig. 12 Influence of Rayleigh number on the average Nusselt number for Pr = 0.7, $0.1 \le S_1/H \le 0.5$, $S_2/H_1 \le 0.6$, and $A \ge 3$

ratio A≥3, Figs.11 and 12 present the variation of the maximum surface temperature and the average Nusselt number of both the bottom and top heaters with tha variation of Rayleigh number $10^4 \le Ra \le 10^7$,

Figure 11 shows that the maximum surface temperature of the upper heater is always higher than that of the lower heater. Therefore, the average Nusselt number for the top heater is always smaller than that of the bootom heater. Tha maximum heater surface temperature and the average Nusselt number for both the upper and lower heaters are correlated as a function of Rayleigh number by equations as follows:

for bottom heater:

$$\theta_{max} = 1.055\ Ra^{-0.139} \quad (8)$$

$$\bar{Nu} = 1.4\ Ra^{0.1179} \quad (9)$$

for top heater:

$$\theta_{max} = 1.4\ Ra^{-0.153} \quad (10)$$

$$\bar{Nu} = 0.99\ Ra^{0.135} \quad (11)$$

To validate the numerical calculated results, experimental tests were done for A=2, W/L=2.5, S_1/H= 0.2, S_2/H_1= 0.29, Pr=0.7 and $Ra=3.2\times10^4$, 1.23×10^5, and 2.65×10^5. Comparison is shown in Fig. 13 between the calculated local surface heated and unheated parts of the wall and the experimental results. Fig. 14 presents also a comparison between the local heater surface Nusselt number with the experimental results calculated from the experimental data according to Eq. 6. Good agreement exists between the predicted and experimental results. The average and maximum error between the predicted and experimental data are 5 and nearly 10 percent, respectively.

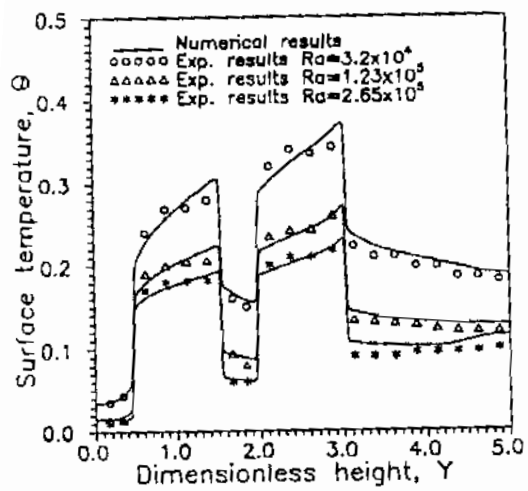

Fig. 13 Comparison between the numerical and experimental surface temperature for A=2, W/L=2.5, Pr=0.7, S_1/H=0.2, S_2/H_1=0.29

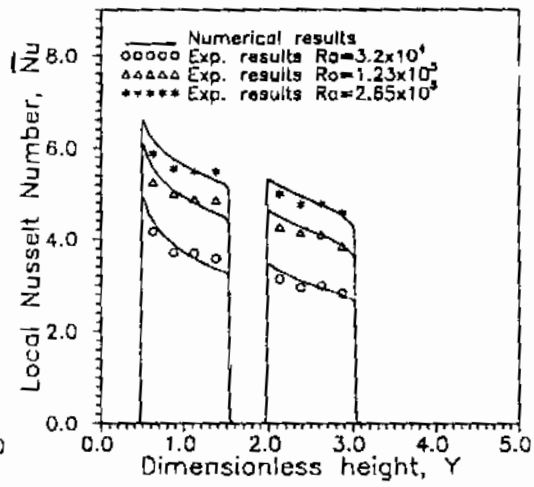

Fig. 14 Comparison between the numerical and experimental heater local Nusselt number for A=2, W/L=2.5, Pr=0.7, S_1/H=0.2, S_2/H_1=0.29

Conclusions

The effect of the wake distance between upper and lower heaters, the enclosure aspect ratio, and Rayleigh number on the flow, heaters surface temperature and heat transfer characteristics are studied numerically. The range of parameters considered is Pr=0.7, lower heater location $0.1 \le S_1/H \le 0.5$, upper heater loeation $0.1 \le S_2/H_1 \le 0.875$, the aspect ratio $1 \le A \le 10$, and $10^4 \le Ra \le 10^7$. The range of parameters for the experimental study is Pr=0.7, A=2, S_1/H=0.2, S_2/H_1= 0.29, W/L=2.5 and Ra=3.2×10^4, 1.23×10^5, and 2.65×10^5. The resnlts show the following conclusions:

The average and maximum surfaee temperatures of the upper heater are always higher than those of the lower heater. Therefore, the local and average Nusselt number for the upper heater are always smaller than those of the lower heater.

For the lower heater both the maximum surface temperature θ_{max} and the average Nusselt nuinber $\bar{N}u$ are not affected by the location of the upper heater and the aspect ratio for $A \ge 3$.

For the upper heater, θ_{max} and $\bar{N}u$ are independent on the aspect ratio for $A \ge 3$, and the upper heater location for $S_2/H_1 \le 0.6$ and the optimum locatiou for the upper heater lies in the lower half of the distauce above the trailing edge of the lower heater where $S_2/H_1 \le 0.6$ and $A \ge 3$.

For the optimum ranges of the lower heater location $0.1 \le S_1/H \le 0.5$, the upper heater location $S_2/H_1 \le 0.6$ and the enclosure aspect ratio $A \ge 3$, the maximum heater surfaee temperature and the average Nusselt number for both the upper and lower heaters are correlated with Rayleigh number as follows:

for bottom heater: $\theta_{max} = 1.055\ Ra^{-0.139}$, $\bar{N}u = 1.4\ Ra^{0.1179}$

for top heater: $\theta_{max} = 1.4\ Ra^{-0.153}$, $\bar{N}u = 0.99\ Ra^{0.135}$

Nomenclature

A	aspeet ratio = H/W
g	gravitational accceleration, m/s^2
H	euclosure height, m
H_1	distanee above the lower heater, m
k	thermal conduetivity, W/mK
L	heater height, m
Nu	local Nusselt number along the heater surface, Eq. (9)
$\bar{N}u$	average Nusselt number, Eq. (10)
P	pressure, Pa
Pr	Prandtle number, ν/α
q	heat flux at the heater surface, W/m^2
Ra	Rayleigh number, $Ra = g \beta L^4 q /(k\alpha\nu)$
S	the height of the lower heater cemter, m
S_1	height of the upper heater eenter above the lower heater trailing edge, m
T	temperature, K

u. v	field velocities in the x and y directions, m/s
U, V	non-dimensional field velocities in the X and Ydirection, uL/v, vL/v
W	enclosure width, m
x, y	distance in horizontal and vertical directions, m
X, Y	dimensionless distance in x direction, x/L and y/L
α	thermal diffusivity eoefficient, m^2/s
β	volumetric coefficient of thermal expansion, 1/K
θ	dimensionless temperature, $(T-T_w)/(q.L/k)$
ψ	stream function, m^2/s
Ψ	nondimensional stream function, ψ/v
ζ	vorticity, 1/s
ω	nondimensional vorticity, $\zeta L^2/v$
ν	kinematic viscosity of the fluid, m^2/s
ρ	fluid density, kg/m^3

References

1. Jaluria, Y., "Natural Convective Cooling of Electronic Equipment," in "Natural convection, Fundamentals & Applications" Kakae, S., Aung, V., and Viskanta, R., Hemisphere Publishing corporation, pp. 961-986, 1985.
2. Incropera, F., P., "Convection Heat Transfer in Electronic Equipment Cooling," ASME J. of Heat Transfer, Vol. 110, pp. 1097-1111, 1988.
3. Papanicolaou, E., and Jaluria, Y., "Mixed Convection From Simulated Electronic Components at Varying Relative Positions in a Cavity," ASME J. of Heat Transfer, Vol. 116, pp. 960-970, 1994.
4. El Kady, M. S., and Araid, F. F., "Natural Convection From a Single Surface Heater in a Vertical Rectangular Enclosure." Mansoura Engineering Journal (MEJ), Vol. 23, No. 2, pp.M -M , June.1998.
5. Habchi, S., and Acharya, S., "Laminar Mixed Convection in a Partially Blocked. Vertical Channel," Int. J. Heat Mass Transfer. Vol. 29, pp. 1711-1722, 1986
6. Kang, B. H., Jaluria, Y., and Tewari, S. S., "Mixed Convection Transport From an Isolated Heat Source Module on a Horizontal Plate." ASME J. of Heat Transfer. Vol. 112, pp. 653-661, 1990.
7. Mahaney, H., Incropera, F., and Ramadhyani, S., "Comparisou of Predicted and Measured Mixed Convection Heat Transfer From an Array of Discrete Sources in a Horizontal Reetangular Channel," Int. J. Heat Mass Transfer, Vol. 33, No. 6, pp. 1233-1245, 1990
8. Kim, S., Sung, H., and Hyun, J., "Mixed Convection From Multiple-Layered Boards With Cross-Streamwise Periodic Boundary Conditions," Int. J. Heat Mass Transfer, Vol. 35, No. 11, pp. 2941-2952, 1992
9. Incropera, F. P., Kerby, J.S., Moffatt, D.F., and Ramadhyani, S., "Conjugate Heat Transfer from Discrete Heat Sources in a Rectangular Channel," Int. J. Heat Mass Transfer. Vol. 29, No. 7, pp. 1051-1058, 1986
10. Davalath J., and Bayazitoglu, Y, "Forced Convection Cooling Across Reetangular Blocks," ASME J. of Heat Transfer, Vol. 109, pp. 321-328, 1987.

11. Kim, S. H., and Anand, N. K., "Turbulent Heat Transfer Between a Series of Parallel Plates With Surface-Mounted Discrete Heat Sources," ASME J. of Heat Transfer, Vol. 116, pp. 577-587, 1994.
12. Kim, S. H., and Anaud, N. K., "Laminar Developing Flow and Heat Transfer Between a Series of Parallel Plates With Surface-Mounted Discrete Heat Sources," Int. J. Heat Mass Transfer, Vol. 37, No. 15, pp. 2231-2244, 1994
13. Kim, S. H., aud Anaud, N. K., "Laminar Heat Transfer Between a Series of Parallel Plates With Surface-Mounted Discrete Heat Sourees," ASME J. of Electronic Packaging , Vol. 117, pp. 52-62, 1995
14. Nakayama, W., and Park, S. H., "Conjugate Heat Transfer From a Single Surface-Mounted Block to Forced Convective Air Flow in a Channel," ASME J. of Heat Transfer, Vol. 118, pp. 301-308, 1996.
15. Jaluria, Y., "Buoyaucy-Induced Flow Due to Isolated Sources on a Vertical Surface," ASME J. of Heat Transfer, Vol. 104, pp. 223-227, 1982.
16. Anand, N., Kim, S., and Aung, W., "Effect of Wall Conduetion of Free Convection Between Asymmetrieally Heated Vertical Plates: Uniform Wall Temperature," Int. J. Heat Mass Transfer, Vol. 33, pp. 1025-1028, 1990.
17. Kim, S., Anand, N., and Aung, W., "Effect of Wall Conduction of Free Convection Between Asymmetrieally Heated Vertical Plates: Uniform Wall Heat Flux," Int. J. Heat Mass Transfer, Vol. 33, pp. 1013-1023, 1990.
18. Kim, S., Anand, N., and Fletcher, L., "Free Convection Between Series of Vertieal Parallel Plates With Embedded Line Heat Sources," ASME J. of Heat Transfer, Vol. 113, pp. 108-115, 1991.
19. Keyhani, M., Prasad, M., and Cox, R., "An Experimental Study of Natural Convection in a Vertieal Cavity with Discrete Heat Sources," ASME J. of Heat Transfer, Vol. 110, pp. 616-624, 1988.
20. Keyhani, M., Chen, L. and Pitts, D., "Aspect Ratio Effect on Natural Convection in an Enclosure With Protruding Heat Sources," ASME J. of Heat Transfer, Vol. 113, pp. 883-891, 1991.
21. Carnuona, R., and Keyhani, M., "The Cavity Width Effect on Iommersion Cooling of Discrete Flush-Heaters on One Vertieal Wall of an Enclosure Cooled From the Top," ASME Journal of Electronic Packaging, Vol. 111, pp. 268-276, 1989.
22. Patankar, S., "Numerical Heat Transfer and Fluid Flow" Mc Graw Hill, New York, 1980.